Journal of Sound and Vibration (2001) **246**(1), 29–46
doi:10.1006/jsvi.2000.3626, available online at http://www.idealibrary.com on IDEAL®

A LOCAL RADIAL POINT INTERPOLATION METHOD (LRPIM) FOR FREE VIBRATION ANALYSES OF 2-D SOLIDS

G. R. Liu and Y. T. Gu

Department of Mechanical and Production Engineering, Centre for Advanced Computations in Engineering Science, National University of Singapore, 10 *Kent Ridge Crescent, Singapore* 119260, *Singapore. E-mails: mpeliugr@nus.edu.sg, engp8973@nus.edu.sg*

(*Received* 8 *November* 2000)

A local radial point interpolation method (LRPIM) is presented to deal with boundary-value problems for free vibration analyses of two-dimensional solids. Local weak forms are developed using weighted residual method locally from the partial differential equation of free vibration. A technique to construct shape functions using radial function basis is proposed. The shape functions so formulated possess delta function property. Essential boundary conditions can be implemented with ease as in the finite-element method. Some important parameters on the performance of LRPIM are also investigated thoroughly. Numerical examples for free vibration analyses of two-dimensional solids to demonstrate the validity and efficiency of the present LRPIM are presented.

1. INTRODUCTION

Meshless method has attracted more and more attention from researchers in recent years, and it is regarded as a potential numerical method in computational mechanics. In the meshless method, it does not require a mesh to discretize the problem domain, and the approximate solution is constructed entirely based on a set of scattered nodes. Several meshless methods, such as diffuse-element method (DEM) [1], element-free Galerkin (EFG) method [2], reproducing kernel particle method (RKPM) [3], point interpolation method (PIM) [4], point assembly method (PAM) [5], boundary node method (BNM) [7] and boundary point interpolation method (BPIM) [6] have been proposed and achieved remarkable progress in solving a wide range of static and dynamic problems. The coupled techniques between meshless methods and other established numerical methods are also developed [8, 9]. The above-mentioned meshless methods are all based on global weak forms or boundary integral equation (BIE). In particular, these meshless methods are "meshless" only in terms of the interpolation of the field or boundary variables, as compared to the usual finite-element method (FEM) or boundary-element method (BEM). These meshless methods have to use background cells to integrate a weak form over the problem domain and boundary.

Two "truly" meshless methods, called the meshless local Petrov–Galerkin (MLPG) method and the local point interpolation method (LPIM), have been developed based on local weak forms. The MLPG [10, 11] method is based on a local weak form and moving least-squares (MLS) approximation. In the MLPG, an integration method in a regular-shaped local domain (such as spheres, rectangular, and ellipsoids) is used. The MLPG method does not need any "element" or "mesh" for both field interpolation and

0022-460X/01/360029 + 18 $35.00/0

background integration. The MLPG method has been used in static [11] and vibration analyses [12] of solids. However, in MLPG method, it is difficult to implement essential boundary conditions and it is computationally expensive due to the use of MLS approximation.

An LPIM has been proposed for two-dimensional solids by Liu and Gu [13], in which a set of points is used to represent the problem domain. A technique to construct polynomial interpolation functions with delta function property is proposed. A local weak form is developed using the weighted residual method locally. The LPIM is also a truly meshless method, in which essential boundary conditions can be implemented as easily as in the FEM due the shape functions having delta function property. The computation cost of LPIM is much lower than that of MLPG because of the simple interpolation and the reduction in computation of the stiffness matrix. The LPIM has been used for 2-D elasto-statics [13] and 1-D fourth order thin beam analyses [14]. Very good results have been obtained.

However, like other methods that use polynomial as basis functions, it is tricky to choose the basis for interpolation in polynomial basis LPIM [15]. If an inappropriate polynomial basis is chosen, it may result in a badly conditioned matrix, which could be even invertible. Some strategies have been developed for alleviating this problem [4, 15]. Using radial functions as the basis in LPIM is a good alternative.

The use of radial basis function for scattered data interpolation began as early as the beginning of 1960s. In recent years, many mathematicians and mechanicians noticed its unique advantages, and used it to solve partial differential equations [16–18]. Using radial basis in LPIM can offer new advantages. A local radial point interpolation method (LRPIM) has been proposed by Liu *et al.* [19]. In LRPIM, the point interpolation using the radial function basis is utilized to construct shape functions with delta function property. The LRPIM can give full play of the advantage of LPIM. In the meantime, the LRPIM overcomes disadvantages of LPIM because the interpolation using radial function basis is stable and flexible. The LRPIM has been for two-dimensional static analyses [19]. Very good results have been obtained.

LRPIM for free vibration analyses of two-dimensional solids and structures are proposed in this paper to extend the LRPIM method to free vibration analyses. Local weak forms are developed using weighted residual method locally from the partial differential equation of free vibration. The point interpolation using radial function basis is used to obtain the shape functions. The shape functions so formulated possess delta function property. Therefore, the essential boundary conditions can be easily implemented in vibration analyses. Frequencies and eigenmodes are obtained by solving an eigenvalue equation.

Programs of the LRPIM have been developed in FORTRAN, and a number of numerical examples of free vibration analyses are presented to demonstrate the convergence, validity and efficiency of the present methods. The effects of some important parameters on the performance of LRPIM are also investigated thoroughly, and the results are presented in detail.

2. POINT INTERPOLATION USING RADIAL FUNCTIONS BASIS

Consider a problem domain Ω. To approximate a function $u(\mathbf{x})$ in Ω, the point interpolant $u^h(\mathbf{x})$ is defined in the domain Ω by

$$u^h(\mathbf{x}) = \sum_{i=1}^{n} B_i(r) a_i + \sum_{j=1}^{m} p_j(\mathbf{x}) b_j(\mathbf{x}) \tag{1}$$

TABLE 1

Typical radial basis functions

Name	Expression	Parameters
Multi-quadrics (MQ)	$B_i(x, y) = (r_i^2 + C)^q$	c, q
Gaussian (Exp)	$B_i(x, y) = \mathrm{e}^{-br_i^2}$	b

with the constraint condition

$$\sum_{i=1}^{n} p_{ij}(x)a_i = 0, \quad j = 1 - m, \tag{2}$$

where $B_i(r)$ is the radial basis function, n is the number of points in the neighborhood of $\mathbf{x}$, $p_j(\mathbf{x})$ is monomials in the space co-ordinates $\mathbf{x}^{\mathrm{T}} = [x, y]$, m is the number of polynomial basis functions and the coefficients a_i and b_j are interpolation constants.

In the radial basis function $B_i(r)$, the variable is only the distance, r, between the interpolation point $\mathbf{x}$ and a node $\mathbf{x}_i$. For a two-dimensional problem, r is defined as

$$r = \sqrt{(x - x_i)^2 + (y - y_i)^2}. \tag{3}$$

There are a number of radial basis functions. The characteristics of radial functions have been widely investigated. As listed in Table 1, the multi-quadrics (MQ) radial function and Gaussian (Exp) radial function are used in this paper. Several parameters need to be determined for each radial basis function. In general, these parameters can be determined by numerical examination. Detailed investigations of these parameters will be given in the following numerical examples.

The second term of equation (1), introduced in this paper, is a polynomial interpolation term. It has been proved that this term can improve interpolation accuracy. In equation (1), only limited number $p_j(\mathbf{x})$ is sufficient, i.e., $m \ll n$. In this paper, the following linear polynomial basis is used:

$$\mathbf{p}^{\mathrm{T}}(\mathbf{x}) = [1, x, y]. \tag{4}$$

Coefficients a_i and b_j in equation (1) can be determined by enforcing equation (1) to be satisfied at the n nodes surrounding point $\mathbf{x}$. Equation (1) can be rewritten in matrix form as

$$\begin{bmatrix} \mathbf{u} \\ \mathbf{0} \end{bmatrix} = \begin{bmatrix} \mathbf{B}_0 & \mathbf{P} \\ \mathbf{P}^{\mathrm{T}} & \mathbf{0} \end{bmatrix} \begin{bmatrix} \mathbf{a} \\ \mathbf{b} \end{bmatrix} = \mathbf{G}\mathbf{a}_0, \tag{5a}$$

where

$$\mathbf{P}^{\mathrm{T}} = \begin{bmatrix} 1 & 1 & \cdots & 1 \\ x_1 & x_2 & \cdots & x_n \\ y_1 & y_2 & \cdots & y_n \end{bmatrix}, \tag{5b}$$

$$\mathbf{B}_0 = \begin{bmatrix} B_1(r_1) & B_2(r_1) & \cdots & B_n(r_1) \\ B_1(r_2) & B_2(r_2) & \cdots & B_n(r_2) \\ \cdots & \cdots & \cdots & \cdots \\ B_1(r_n) & B_2(r_n) & \cdots & B_n(r_n) \end{bmatrix}, \tag{5c}$$

$$\mathbf{a}_0^{\mathrm{T}} = [a_1, a_2, \ldots, a_n, b_1, b_2, b_3,]. \tag{5d}$$

Hence, we have

$$u(\mathbf{x}) = \mathbf{\Phi}(\mathbf{x})\mathbf{u}_e, \tag{6a}$$

where the shape function $\mathbf{\Phi}(\mathbf{x})$ is defined by

$$\mathbf{\Phi}(\mathbf{x}) = [B_1(r) \quad B_2(r) \quad \cdots \quad B_n(r) \quad 1 \quad x \quad y]\mathbf{G}^{-1} \tag{6b}$$

and

$$\mathbf{u}_e^{\mathrm{T}} = [u_1 \quad u_2 \quad \cdots \quad u_n \quad 0 \quad 0 \quad 0]. \tag{6c}$$

The shape function $\mathbf{\Phi}(\mathbf{x})$ obtained through the above procedure possesses delta function properties, i.e.,

$$\phi_i(\mathbf{x}_j) = \delta_{ij} = \begin{cases} 1, & i = j, \\ 0, & i \neq j. \end{cases} \tag{7}$$

Mathematicians have proved the existence of $\mathbf{B}_0^{-1}$ for arbitrary scattered nodes [20, 21]. In addition, the order of polynomial in equation (1) is lower (only linear in this paper). Therefore, in general, $\mathbf{G}^{-1}$ (in equation (6b)) exists.

3. LOCAL WEAK FORM OF LRPIM

The governing equation for no damping free vibration is as follows:

$$m\ddot{u}_i + \sigma_{ij,j} = 0, \tag{8}$$

where m is the mass density, $\ddot{u}_i = \partial^2 u_i/\partial t^2$ is the acceleration, σ_{ij} the stress tensor, which corresponds to the displacement field u_i, and $(\,)_j$ denotes $\partial/\partial x_j$. The auxiliary conditions are given as follows:

$$\textit{Natural boundary condition}: \quad \sigma_{ij}n_j = \bar{t}_i = 0 \quad \text{on } \Gamma_t, \tag{9a}$$

$$\textit{Essential boundary condition}: \quad u_i = \bar{u}_i \quad \text{on } \Gamma_u, \tag{9b}$$

in which the $\bar{u}_i$, $\bar{t}_i$, denote the prescribed displacements, tractions, respectively, and n_j is the unit outward normal to domain Ω. For free vibration analysis, the essential boundary conditions are always homogeneous.

In the free vibration analysis, $\mathbf{u}(\mathbf{x}, t)$ can be written as

$$\mathbf{u}(\mathbf{x}, t) = \mathbf{u}(\mathbf{x})\sin(\omega t + \varphi), \tag{10}$$

where ω is the frequency. Substituting equation (10) into equation (8) leads to the following equations:

$$\sigma_{ij,j} - \omega^2 m u_i = 0. \tag{11}$$

It should be noted that the stresses, $\boldsymbol{\sigma}$, and displacements, $\mathbf{u}$, in equation (11) are only the function of co-ordinator $\mathbf{x}$.

A local weak form of equation (11), over a local sub-domain Ω_s bounded by Γ_s, can be obtained using the weighted residual method

$$\int_{\Omega_s} w_i(\sigma_{ij,j} - \omega^2 m u_i)\,\mathrm{d}\Omega = 0, \tag{12}$$

where w_i is the weight function.

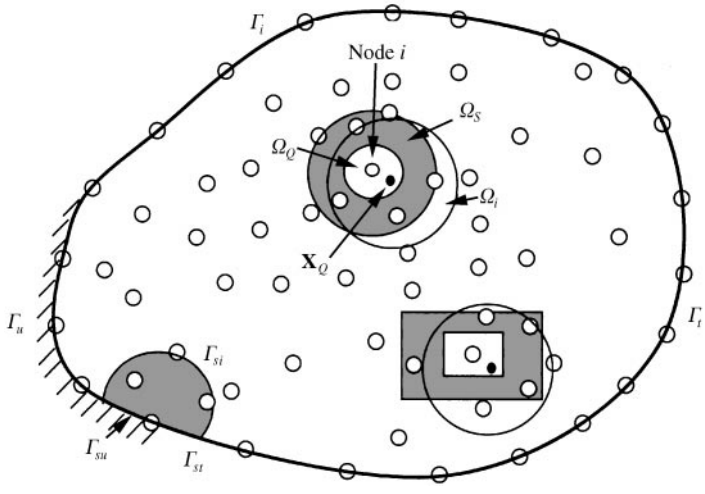

Figure 1. The support domain Ω_s and integration domain Ω_Q for node i; the interpolation domain Ω_i for Gauss integration point $\mathbf{x}_Q$.

The first term on the left-hand side of equation (16) can be integrated by parts to become

$$\int_{\Gamma_s} w_i \sigma_{ij} n_j \, \mathrm{d}\Gamma - \int_{\Omega_s} (w_{i,j}\sigma_{ij} + w_i \omega^2 m u_i) \, \mathrm{d}\Omega = 0. \tag{13}$$

The support sub-domain Ω_s of a node $\mathbf{x}_i$ is a domain in which $w_i(x) \neq 0$. An arbitrary shape support domain can be used. A circle or rectangular support domain is used in this paper for convenience. From Figure 1, it can be found that the boundary Γ_s for the support domain is usually composed of three parts: the internal boundary Γ_{si}, the boundaries Γ_{su} and Γ_{st}, over which the essential and natural boundary conditions are specified. Imposing the natural boundary condition and noting that $\sigma_{ij} n_j = \partial u/\partial n \equiv t_i$ in equation (13), we obtain

$$\int_{\Gamma_{si}} w_i t_i \, \mathrm{d}\Gamma + \int_{\Gamma_{su}} w_i t_i \, \mathrm{d}\Gamma + \int_{\Gamma_{st}} w_i \bar{t}_i \, \mathrm{d}\Gamma - \int_{\Omega_s} (w_{i,j}\sigma_{ij} + w_i \omega^2 m u_i) \, \mathrm{d}\Omega = 0. \tag{14}$$

For a support domain located entirely within the global domain, there is no intersection between Γ_s and the global boundary Γ, $\Gamma_{si} = \Gamma_s$, and the integrals over Γ_{su} and Γ_{st} vanish. In the free vibration analysis, the integrals over Γ_{st} vanish for all nodes because of $\bar{t} = 0$ on Γ_t.

With equation (14) for any node $\mathbf{x}_i$, instead of dealing with a global problem equation (11), the problem becomes to deal with a localized problem over a local support domain. Theoretically, as long as the union of all local domains, Ω_s, covers the global domain Ω, the equilibrium equation and the boundary conditions will be satisfied in the global domain Ω and in its boundary Γ by using above-discussed LRPIM [10]. However, the support domain used will affect the solution. The influence of the choice of local support domain will be studied in detail in the following numerical examples.

4. DISCRETIZATION AND NUMERICAL IMPLEMENTATION FOR THE LRPIM

4.1. DISCRETE EQUATION OF LRPIM

The problem domain Ω is represented by properly scattered nodes. The point interpolation approximation (6) is used to approximate the value of a point $\mathbf{x}_Q$. Substituting equation (6) into the local weak form (14) for all nodes leads to the following discrete system equations:

$$\mathbf{Ku} - \omega^2 \mathbf{Mu} = 0, \tag{15}$$

where the "stiffness" matrix $\mathbf{K}$ and "mass" matrix $\mathbf{M}$ are defined by

$$\mathbf{K}_{ij} = \int_{\Omega_s} \mathbf{v}_i^{\mathrm{T}} \mathbf{D}\mathbf{B}_j \, \mathrm{d}\Omega - \int_{\Gamma_{si}} \mathbf{w}_i \mathbf{N}\mathbf{D}\mathbf{B}_j \, \mathrm{d}\Gamma - \int_{\Gamma_{su}} \mathbf{w}_i \mathbf{N}\mathbf{D}\mathbf{B}_j \, \mathrm{d}\Gamma, \tag{16a}$$

$$\mathbf{M}_{ij} = \int_{\Omega} m \mathbf{w}_i \mathbf{\Phi}_j \, \mathrm{d}\Omega \tag{16b}$$

with $\mathbf{w}$ being the value of the weight function matrix, $\mathbf{\Phi}$ the shape function matrix, corresponding to node i, evaluated at the point $\mathbf{x}$, and

$$\mathbf{N} = \begin{bmatrix} n_x & 0 & n_y \\ 0 & n_y & n_x \end{bmatrix}, \qquad \mathbf{B}_j = \begin{bmatrix} \phi_{j,x} & 0 \\ 0 & \phi_{j,y} \\ \phi_{j,y} & \phi_{j,x} \end{bmatrix}, \tag{16c, d}$$

$$\mathbf{v}_i = \begin{bmatrix} w_{i,x} & 0 \\ 0 & w_{i,y} \\ w_{i,y} & w_{i,x} \end{bmatrix}, \tag{16e}$$

$$\mathbf{D} = \begin{bmatrix} 1 & v & 0 \\ v & 1 & 0 \\ 0 & 0 & (1-v)/2 \end{bmatrix} \text{ for plane stress.} \tag{16f}$$

For free vibration analyses, equation (15) can also be written as

$$(\mathbf{K} - \omega^2 \mathbf{M})\mathbf{q} = 0, \tag{17}$$

where $\mathbf{q}$ is the eigenvector. In order to determine the frequencies, ω, and free vibration modes, it is necessary to solve the eigenvalue equation (17). The essential boundary condition (9b), can be easy to implement in the same way in the FEM due to shape functions possessing delta function property.

4.2. NUMERICAL IMPLEMENTATION FOR LRPIM

As the MLPG is regarded as a weighted residual method, the weight function plays an important role in the performance of the method. Theoretically, as long as the condition of continuity is satisfied, any weight function is acceptable. However, the local weak form is

based on the local sub-domains centered by nodes. It can be found that the weight function with the local property, which should decrease in magnitude as the distance from a point $\mathbf{x}_Q$ to the node $\mathbf{x}_i$ increases, yields better results. Therefore, we will consider weight functions, which only depend on the distance between two points. The following spline weight functions is used in this paper:

$$w_i(x) = \begin{cases} 1 - 6\left(\dfrac{d_i}{r_w}\right)^2 + 8\left(\dfrac{d_i}{r_w}\right)^3 - 3\left(\dfrac{d_i}{r_w}\right)^4, & 0 \leqslant d_i \leqslant r_w, \\ 0, & d_i \geqslant r_w, \end{cases} \tag{18}$$

where $d_i|\mathbf{x}_Q - \mathbf{x}_i|$ is the distance from node $\mathbf{x}_i$ to the sampling point $\mathbf{x}_Q$ and r_w is the size of the support for the weight function.

It can be easily seen that the system stiffness matrix $\mathbf{K}$ in the present method is banded but usually asymmetric. However, similar to the Galerkin FE methods, the weight function, w, can be taken as the same formulation as equation (6). In this case, $\mathbf{K}$ becomes symmetrical [10]. This symmetrical stiffness matrix can be an added advantage in applying the present LRPIM method.

A numerical integration is needed to evaluate the integration in equation (16). The Gauss quadrature is used in the LRPIM. For a node $\mathbf{x}_i$, a local integration cell is needed to employ Gauss quadrature. For each Gauss quadrature point $\mathbf{x}_Q$, the point interpolation is performed to obtain the integrand. Therefore, as shown in Figure 1, for a node $\mathbf{x}_i$, there exist three local domains: local integration domain Ω_Q (size r_q), weight function domain Ω_w (same as Ω_s) for $w_i \neq 0$ (size r_w), and interpolation domain Ω_i for x_Q (size r_i). These three local domains are independent as long as the condition $r_q \leqslant r_w$ is satisfied. It should be noted that when the weight function (18) is used, the weight function w will be zero along the boundary of integration domain if the integration domain and weight domain are same ($r_q = r_w$). Equation (16b) can be simplified because the integration along the internal boundary Γ_{si} vanishes. Hence, for simplification, we take $r_q = r_w$ in this paper. Since the problem domains in the following examples are rectangle domains, rectangle sub-domains are used for establishing weight function. The size of the sub-domain (r_w) for node i and the size of the interpolation domain (r_i) are defined as

$$r_w = \alpha d_i, \qquad r_i = \beta d_i, \tag{19a, b}$$

where α and β are the coefficients chosen. The d_i is the shortest distance between the node i and neighbor nodes. The effects of α and β will be investigated in the following numerical examples.

There exist difficulties to obtain the exact numerical integration in meshless methods [10]. An insufficiently accurate numerical integration may cause deterioration and rank deficiency in the numerical solution. The numerical integration errors are results from the complexities of the integrand. First, the shape functions constructed using the point interpolation have a complex feature. The shape functions have different forms in each small integration region. The derivatives of shape functions might have an oscillation. Second, the overlapping of interpolation domains makes the integrand in the overlapping domain very complicated. In order to guarantee the accuracy of the numerical integration, the Ω_Q should be divided into some regular small partitions. In each small partition, more Gauss quadrature points should be used [13].

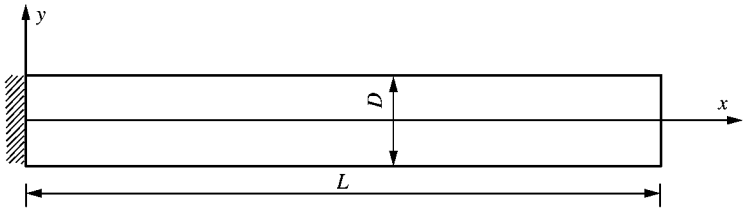

Figure 2. Cantilever beam.

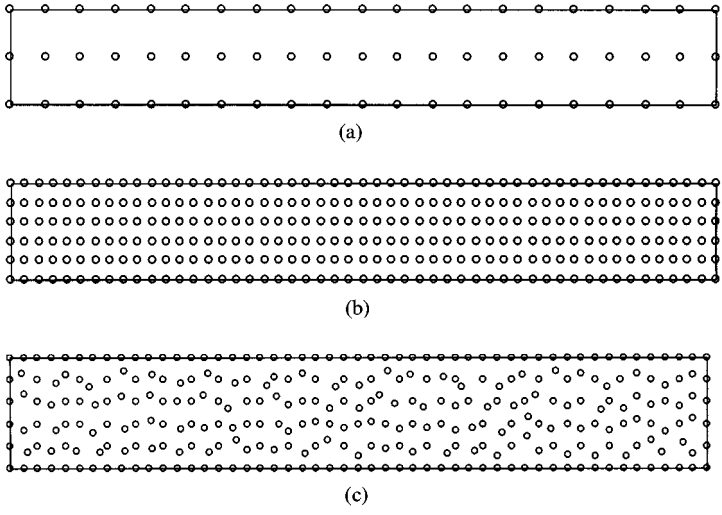

Figure 3. Nodal distribution of the beam: (a) coarse nodal distribution; (b) regular fine nodal distribution; and (c) irregular fine nodal distribution.

5. NUMERICAL RESULTS

The present LRPIM is used for free vibration analyses of 2-D solids. Except specially mentioned, the units are taken as standard international (SI) units in the following examples.

5.1. A CANTILEVER BEAM

The LRPIM method is first applied to analyze free vibration of a cantilever beam as shown in Figure 2. The problem has been analyzed by Nagashima [22] using another meshless method, the node-by-node meshless (NBNM) method, which is based on a global weak form and the MLS approximation. A plane stress problem is considered. The parameters are taken as length $L = 100$ mm, height $D = 10$ mm, thickness $t = 1{\cdot}0$ mm, Young's modulus $E = 2{\cdot}1 \times 10^4$ kgf/mm^2, the Poisson ratio $v = 0{\cdot}3$, mass density $m = 8{\cdot}0 \times 10^{-10}$ kgfs^2/mm^4. Figure 3 shows three kinds of nodal arrangements, coarse (63 nodes) arrangement, fine arrangement with regular and irregular distributed 306 nodes. Parameters on the performance of the present method are investigated first. In the following

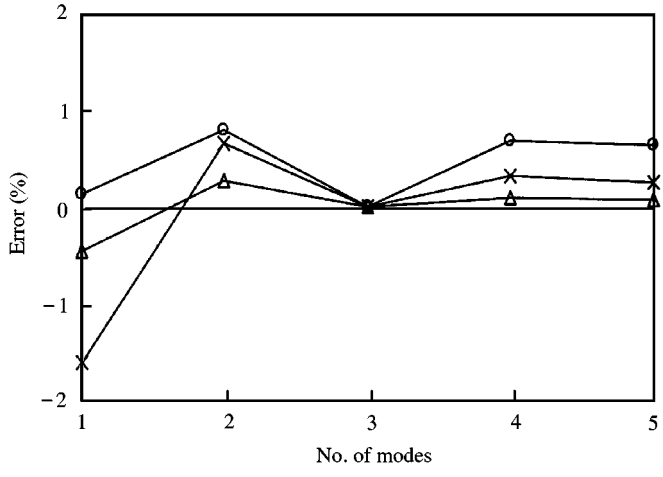

Figure 4. Influence of parameter q of MQ on frequencies: —○—, $q = -0{\cdot}5$; —△—, $q = 1{\cdot}03$; —×—, $q = 0{\cdot}5$.

parameter investigations, regular distributed 306 nodes (Figure 3(b)) are used. As reference, results are obtained by FEM software (ABAQUS) using a very fine mesh with 8000 degrees of freedom (d.o.f.).

5.1.1. *Effects of radial function parameters*

Both multi-quadrics (MQ) radial function and Gaussian (Exp) radial function are used as basis function in this paper. As shown in Table 1, some parameters (C and q for MQ, b for Exp) will influence the performance of these radial functions [16–18]. C is defined as

$$C = \sqrt{c_0 d_i}, \tag{20}$$

where c_0 is the coefficient chosen. The d_i is the shortest distance between the node i and neighbor nodes.

(a) *Effect of C and q for* MQ. In static analyses, it has been found that parameter q influences the performance of MQ more importantly than parameter C. Therefore, q is investigated first. $q = 0{\cdot}5$ and $-0{\cdot}5$ are the traditional parameters in MQ [16–18]. The parameter of $q = 1{\cdot}03$ was first discovered and examined by Liu *et al.* [19]. Natural frequencies for $q = -0{\cdot}5$, $0{\cdot}5$ and $1{\cdot}03$ are obtained and compared with the FEM result. Errors for different q are plotted in Figure 4. From Figure 4, it can be observed that $q = 1{\cdot}03$ leads to a better result in the range of studies. Hence, $q = 1{\cdot}03$ is used in the following studies.

It has been found that very small or big values of C should not be taken [19]. Therefore, c_0 in equation (20) is taken as $1{\cdot}0$, $2{\cdot}0$ and $4{\cdot}0$ respectively. Errors in the results of natural frequency are plotted in Figure 5. From Figure 5, we can find that the influence of parameter C is smaller than q. For convenience, $c_0 = 1{\cdot}0$ will be used in the following studies.

(b) *Effect of b for Exp.* There is only one parameter b in the Exp radial function. For comparison, b is taken as $0{\cdot}3$, $0{\cdot}03$ and $0{\cdot}003$. Error in the results of natural frequency are plotted in Figure 6. From this figure, one can observe that a better accuracy can be obtained for a smaller b. However, a smaller b leads to a larger condition number in the system matrix due to the property of the Exp radial function. In our studies, it is found that

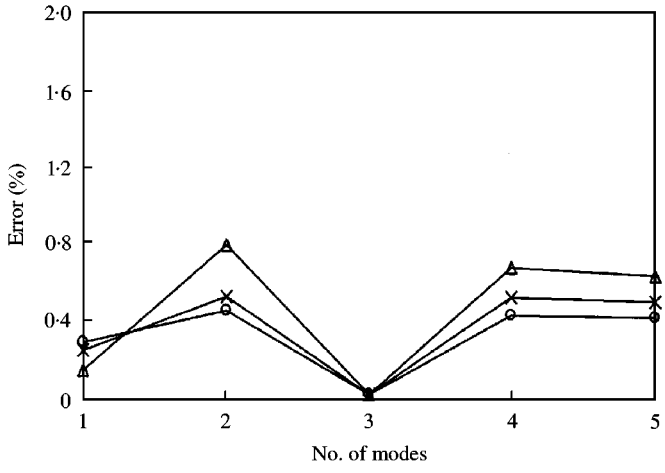

Figure 5. Influence of parameter c_0 of MQ on frequencies: —○—, $c_0 = 1{\cdot}0$; —×—, $c_0 = 2{\cdot}0$; —△—, $c_0 = 4{\cdot}0$.

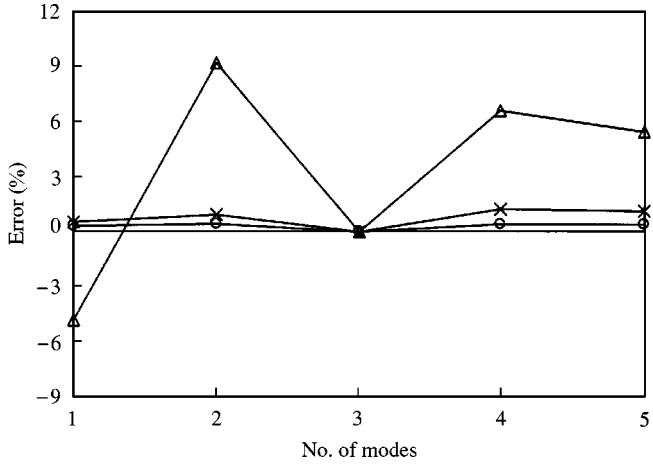

Figure 6. Influence of parameter b of Exp on frequencies: —○—, $b = 0{\cdot}003$; —×—, $b = 0{\cdot}03$; —△—, $b = 0{\cdot}3$.

$b = 0{\cdot}003$ will lead to an ill-conditioned matrix when a big influence domain is used ($\beta \geqslant 3{\cdot}5$ in equation (19b)). $b = 0{\cdot}03$ is robust and with acceptable accuracies in the range of cases studied. $b = 0{\cdot}03$ will be used in the following studies.

5.1.2. *Effects of local support domain*

As the LRPIM is a local meshless method, the size of the local support domain used will affect the accuracy of the solution. Several support domains with different sizes are therefore investigated. The errors of the frequencies for the first three modes are plotted in Figure 7. From this figure, it can be found that the accuracy for frequencies increases with the increase of the support domain size for both MQ and Exp basis.

When the support domain is too small ($\alpha = 0{\cdot}5$), the results will become unacceptable. This is because a local residual formulation with very small support domain for the weight function behaves more like a strong form formulation [23]. Strong form formulation is

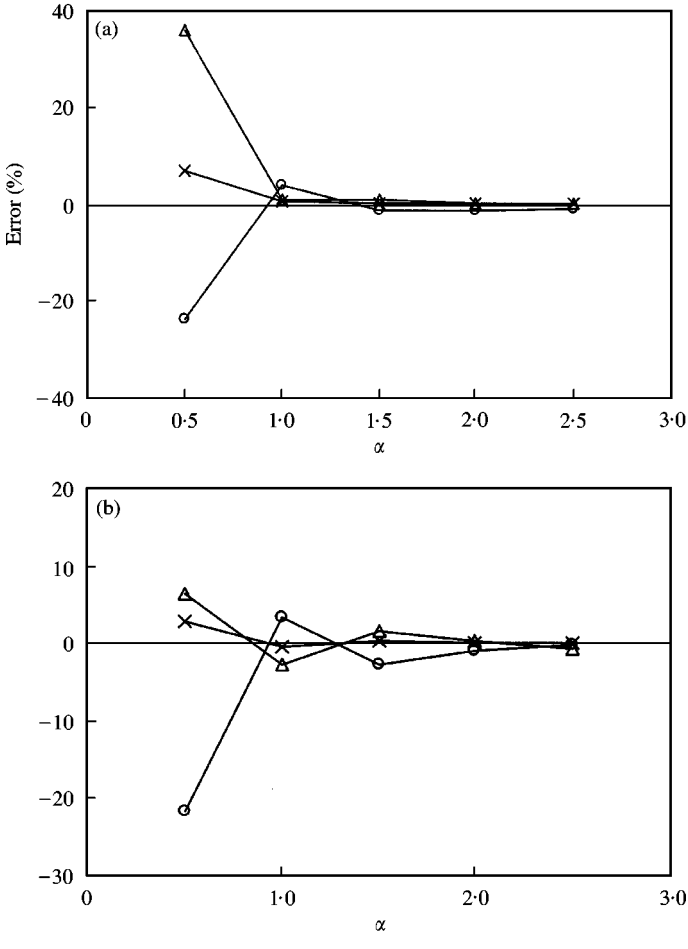

Figure 7. Influence of parameter α of the support domain on frequencies. (a) LRPIM (MQ), (b) LRPIM (Exp): —○—, mode 1; —△—, mode 2; —×—, mode 3.

usually less accurate than a weak integral form formulation, where integration smears the error over the integral domain.

When the support domain is big enough ($\alpha \geqslant 1{\cdot}5$), the results obtained are very good. However, there exist difficulties to get accurate numerical integrations for a big sub-support domain. More regular small partitions and Gauss quadrature points are needed. The numerical integration for a big sub-support domain becomes computationally expensive and is not really necessary. Hence, $\alpha = 2{\cdot}0$ is an economic choice.

It may also be mentioned here that very large local support domain does not necessarily provide a significant improvement on accuracy. This fact is clearly evidenced in Figure 7. This fact implies that as long as the integral domain is large enough to "smear" error, the size of the integral domain does not play an important role.

5.1.3. *Effects of interpolation domain*

The size of influence domain of a quadrature point is decided by the parameter β in equation (19b). Since the problem domain is rectangular, rectangular influence domains are

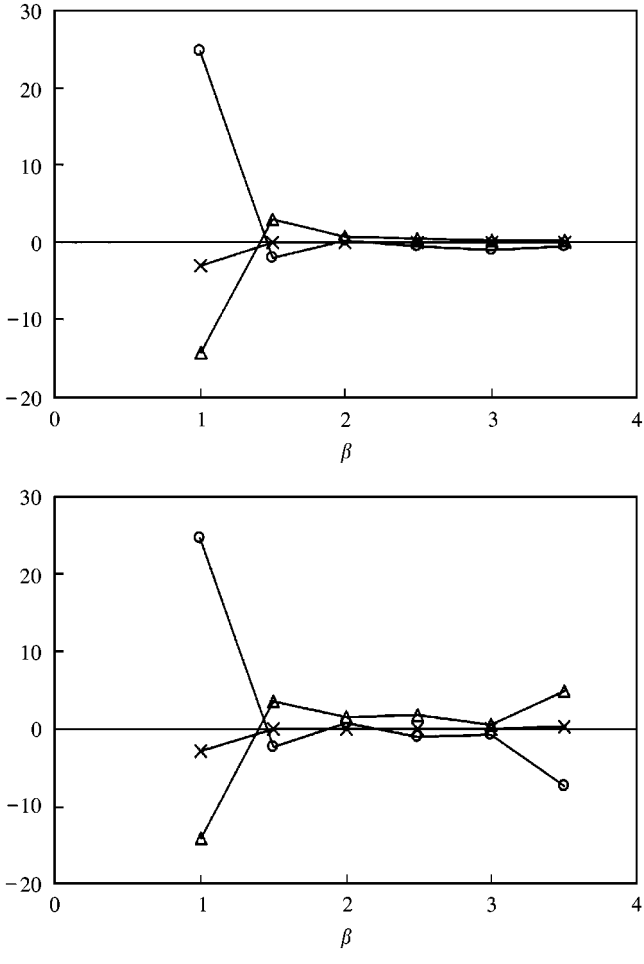

Figure 8. Influence of parameter β of the influence domain on frequencies. (a) LRPIM (MQ), (b) LRPIM (Exp): —○—, mode 1; —△—, mode 2; —×—, mode 3.

used. Results of $\beta = 1{\cdot}0–3{\cdot}5$ are obtained and plotted in Figure 8. It can be found that results of $\beta = 1{\cdot}5–3{\cdot}0$ (about 15–40 nodes used in an influence domain) are very good. A very small influence domain ($\beta = 1{\cdot}0$) and a very big influence domain ($\beta > 3{\cdot}5$) lead to big errors. The poor accuracy of a very small influence domain is because there are not enough nodes (about less than eight nodes) to perform interpolation for the field variable. On the contrary, a very big influence domain will increase the numerical error of interpolation because there are too many nodes (about more than 70 nodes) to perform interpolation. Therefore, $\beta = 1{\cdot}5–3{\cdot}0$ can obtain an acceptable result. For convenience and consistency, $\beta = 2{\cdot}0$ will be used in the following studies.

5.1.4. *Modal analyses results of the beam*

Using the above-mentioned parameters, frequencies of two regular distributed nodal arrangements obtained by LRPIM are listed in Table 2. The results obtained by NBNM method [22] and a commercial FEM software, ABAQUS, using rectangular elements with same number of nodes are listed in the same table. From this table, one can observe that the

TABLE 2

Natural frequency (Hz) of a cantilever beam with different regular nodal distributions

	Coarse node distribution (63 nodes)				Fine node distribution (306 nodes)				
Mode	LRPIM (MQ)†	LRPIM (Exp)‡	Nagashima [22]	FEM (ABAQUS)	LRPIM (MQ)†	LRPIM (Exp)‡	Nagashima [22]	FEM (ABAQUS)	FEM (8000 d.o.f.)
1	888·6	1000·3	926·10	870	824·3	825·8	844·19	830	823
2	5309·6	5034·0	5484·11	5199	4976·6	4958·4	5051·21	4979	4937
3	12829·4	12781·1	12831·88	12 830	12826·5	12826·0	12827·60	12 826	12 824
4	13963·9	13643·8	14201·32	13 640	13093·5	13058·3	13258·21	13 111	13 005
5	25311·2	24993·0	25290·04	24 685	23781·9	23726·3	23992·82	23 818	23 632
6	38463·2	38234·5	37350·18	37 477	36258·3	36179·8	36432·15	36 308	36 040
7	38488·0	38324·5	38320·59	38 378	38451·6	38450·2	38436·43	38 436	38 442
8	52832·6	52727·1	50818·64	51 322	49910·7	49806·8	49937·19	49 958	49 616
9	64012·4	63806·1	63283·70	63 584	63987·8	63985·6	63901·16	63 917	63 955
10	67933·3	68087·4	63994·48	65 731	64334·8	64202·9	64085·90	64 348	63 967

†MQ: $q = 1{\cdot}03$, $c_0 = 1{\cdot}0$, $\alpha = 2{\cdot}0$, $\beta = 2{\cdot}0$.
‡Exp: $b = 0{\cdot}03$, $\alpha = 2{\cdot}0$, $\beta = 2{\cdot}0$.

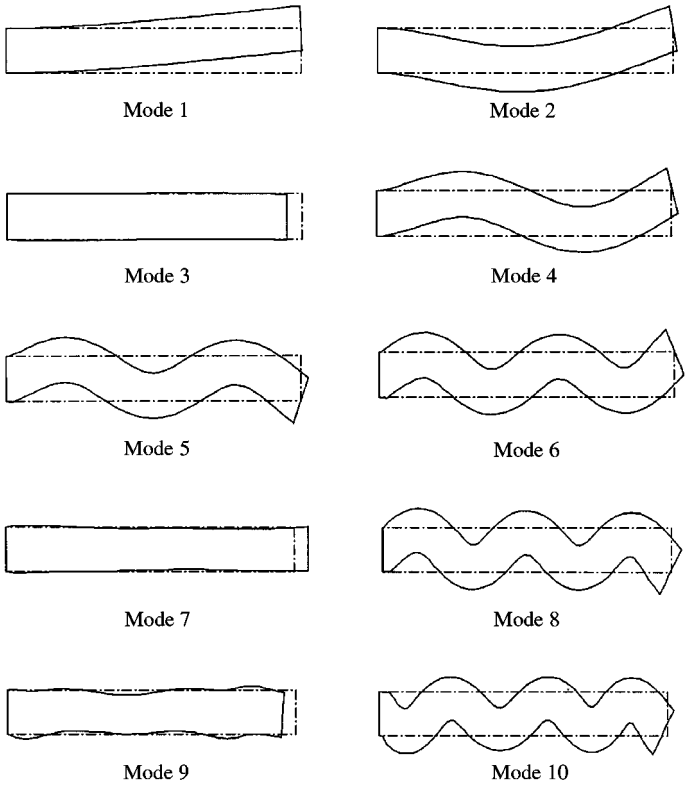

Figure 9. Eigenmodes for the cantilever beam by LRPIM method.

results of the present LRPIM method are in very good agreement with those obtained using FE and NBNM methods. The convergence of the present method is also demonstrated in Table 2. As the number of nodes increases, results obtained by the present LRPIM approach the FEM results with extremely fine mesh, which serves as reference. The first 10 eigenmodes obtained by LRPIM method are plotted in Figure 9. Comparing with FEM results and Nagashima's [22] results, almost identical results are obtained. The results indicate that the LRPIM is as good as those of FEM, which can be considered as a whole domain residual method. We, therefore, emphasize again that the size of the local integral domain in the local residual weak form is not important when it is larger than a certain size.

The irregular distribution nodal arrangement, shown in Figure 3(c), is also used for the modal analysis. Frequencies results are listed in Table 3. From Table 3, one can observe that very good results are obtained using the irregular distribution nodal arrangement. The computational stability and high accuracy for a non-structured nodal distribution are very significant advantages of LRPIM. These properties are very beneficial for practical applications of LRPIM.

5.2. A SHEAR WALL

Figure 10 shows a shear wall with four openings, which has been solved using boundary element method by Brabbia *et al.* [24]. The problem is solved for the plane stress case with

TABLE 3

Natural frequency (Hz) of a cantilever beam with irregular nodal distribution

Mode	LRPIM (MQ)†	Error (%)	LRPIM (Exp)‡	Error (%)	Nagashima [22]	Error (%)	FEM (ABAQUS)	Error (%)	FEM (8000 d.o.f.)
1	820·2	− 0·349	815·0	− 0·987	844·19	2·565	830	0·841	823
2	4938·4	0·018	4982·8	0·918	5051·21	2·303	4979	0·841	4937
3	12814·3	− 0·076	12815·7	− 0·065	12827·60	0·028	12 826	0·016	12 824
4	13005·0	0·000	13078·3	0·563	13258·21	1·947	13 111	0·815	13 005
5	23652·2	0·086	23724·0	0·389	23992·82	1·527	23 818	0·787	23 632
6	36096·7	0·157	36230·0	0·527	36432·15	1·088	36 308	0·744	36 040
7	38418·8	− 0·060	38423·9	− 0·047	38436·43	− 0·014	38 436	− 0·016	38 442
8	49742·9	0·256	49912·5	0·598	49937·19	0·647	49 958	0·689	49 616
9	63919·6	− 0·055	63938·5	− 0·026	63901·16	− 0·084	63 917	− 0·059	63 955
10	64198·3	0·362	64419·2	0·707	64085·90	0·186	64 348	0·596	63 967

†MQ: $q = 1{\cdot}03$; $c_0 = 1{\cdot}0$, $\alpha = 2{\cdot}0$, $\beta = 2{\cdot}0$.
‡Exp: $b = 0{\cdot}03$, $\alpha = 2{\cdot}0$, $\beta = 2{\cdot}0$.

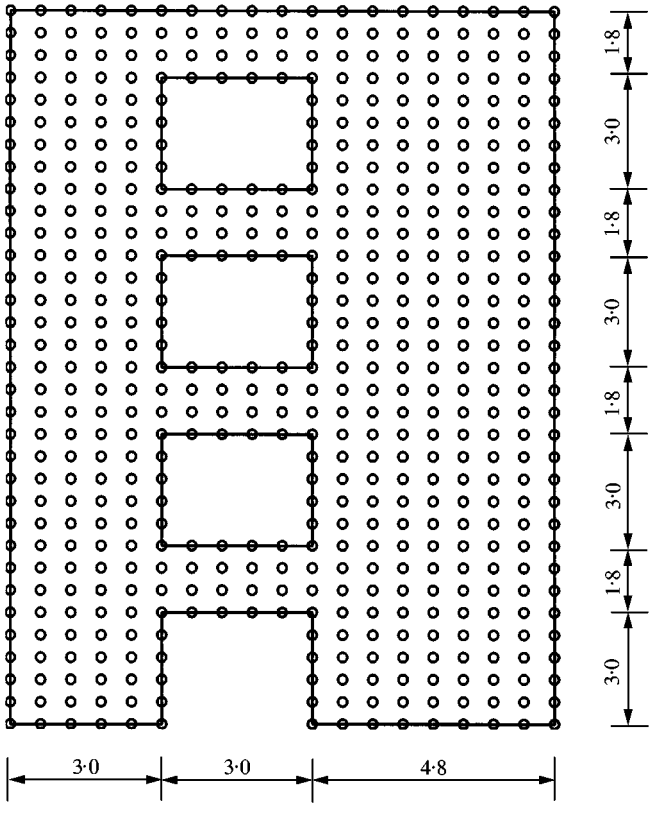

Figure 10. A shear wall with four openings.

TABLE 4

Natural frequencies of a shear wall

	ω (rad/s)			
Mode	LRPIM (MQ)†	LRPIM (Exp)‡	FEM (ABAQUS)	Brabbia [24]
1	2·086	2·090	2·073	2·079
2	7·152	7·133	7·096	7·181
3	7·647	7·645	7·625	7·644
4	12·019	11·987	11·938	11·833
5	15·628	15·617	15·341	15·947
6	18·548	18·508	18·345	18·644
7	20·085	20·087	19·876	20·268
8	22·564	22·518	22·210	22·765

†MQ: $q = 1{\cdot}03$, $c_0 = 1{\cdot}0$, $\alpha = 2{\cdot}0$, $\beta = 2{\cdot}0$.
‡Exp: $b = 0{\cdot}03$, $\alpha = 2{\cdot}0$, $\beta = 2{\cdot}0$.

$E = 1000$, $v = 0{\cdot}2$, $t = 1{\cdot}0$ and $m = 1{\cdot}0$. A total of 574 uniformed nodes are used to discretize the problem domain. The problem is also solved using FEM software ABAQUS. Natural frequencies of the first eight modes are calculated and listed in Table 4. The results obtained by the present LRPIM are in very good agreement with those obtained using BEM and FEM.

6. DISCUSSION AND CONCLUSIONS

A local radial point interpolation method (LRPIM) for free vibration analyses of two-dimensional solids and structures have been presented in this paper. Local weak forms are developed using weighted residual method locally from the partial differential equation of the free vibration. The point interpolation using radial functions as the basis is used to obtain the shape functions. The shape functions so formulated possess delta function property. Therefore, the essential boundary conditions can be easily implemented in free vibration analyses. Some important parameters on the performance of the present method are investigated in great detail. From the studies in this paper, the following conclusion can be drawn:

(1) Using radial function basis in the LRPIM, the point interpolation becomes stable and flexible for both regular and irregular nodal distributions.
(2) For MQ radial function, $q = 1{\cdot}03$ and $c_0 = 1{\cdot}0$, and for Exp radial function, $b = 0{\cdot}03$ leads to acceptable results for most problems studied.
(3) When the local support domain is big enough ($\alpha \geqslant 1{\cdot}5$), the results obtained are very good. $\alpha = 2{\cdot}0$ is recommended.
(4) The size of influence domain of $\beta = 1{\cdot}5$–$3{\cdot}0$ should be used for most problems studied.
(5) Numerical examples of free vibration analyses are presented to demonstrate the convergence, validity and efficiency of the present method. The results presented are indeed very encouraging. It is demonstrated that the LRPIM is easy to implement, and very flexible for free vibration analyses in solids and structures.

REFERENCES

1. B. NAYROLES, G. TOUZOT and P. VILLON 1992 *Computational Mechanics* **10**, 307–318. Generalizing the finite element method: diffuse approximation and diffuse elements.
2. T. BELYTSCHKO, Y. Y. LU and L. GU 1994 *International Journal for Numerical Methods in Engineering* **37**, 229–256. Element-free Galerkin methods.
3. W. K. LIU, S. JUN and Y. F. ZHANG 1995 *International Journal for Numerical Methods in Engineering* **20**, 1081–1106. Reproducing kernel particle methods.
4. G. R. LIU and Y. T. GU 2001 *International Journal for Numerical Methods in Engineering* **50**, 937–951 A point interpolation method for two-dimensional solids.
5. G. R. LIU 1999. *Impact Response of Materials & Structures* (V. P. W. Shim, editors), 475–480. Oxford, New York. A point assembly method for stress analysis for solid.
6. M. K. CHATI and S. MUKHERJEE S 2000 *International Journal for Numerical Methods in Engineering* **47**, 1523–1547. The boundary node method for three-dimensional problems in potential theory.
7. Y. T. GU and G. R. LIU 2000 *Computational Mechanics*. A boundary point interpolation method for stress analysis of solids. In press.
8. T. BELYTSCHKO and D. ORGAN 1995 *Computational Mechanics* **17**, 186–195. Coupled finite-element–element-free Galerkin method.
9. G. R. LIU and Y. T. GU 2000 *Computational Mechanics* **26**, 166–173. Coupling element free Galerkin and hybrid boundary element methods using modified variational formulation.
10. S. N. ATLURI, H. G. KIM and J. Y. CHO 1999 *Computational Mechanics* **24**, 348–372. A critical assessment of the truly meshless local Petrov–Galerkin (MLPG), and local boundary integral equation (LBIE) methods.
11. S. N. ATLURI and T. ZHU 2000 *Computational Mechanics* **25**, 169–179. The meshless local Petrov–Galerkin (MLPG) approach for solving problems in a elasto-statics.
12. Y. T. GU and G. R. LIU 2001 *Computational Mechanics* **27**, 188–198 . A meshless local Petrov–Galerkin (MLPG) method for free and forced vibration analyses for solids.
13. G. R. LIU and Y. T. GU 2001 *International Journal of Structural Engineering and Mechanics* **11**, 221–236. A local point interpolation method for stress analysis of two-dimensional solids.

14. Y. T. GU and G. R. LIU 2001 *Computer Methods in Applied Mechanics and Engineering* **190**, 5515–5528. A local point interpolation method (LPIM) for static and dynamic analysis of thin beams.
15. J. G. WANG, G. R. LIU and Y. G. WU 2000 *Comunications in Numerical Methods in Engineering* (*revised*). Several numerical problems in point interpolation method.
16. E. J. KANSA 1990 *Computers & Mathematics with Applications* **19**, 127–145. Multiquadrics—a scattered data approximation scheme with applications to computational fluid dynamics.
17. C. FRANKE and R. SCHABACK 1997 *Applied Mathematics and Computation* **93**, 73–82. Solving partial differential equations by collocation using radial basis functions.
18. M. SHARAN, E. J. KANSA and S. GUPTA 1997 *Applied Mathematics and Computation* **84**, 275–302. Application of the multiquadric method for numerical solution of elliptic partial differential equations.
19. G. R. LIU, L. YAN and J. G. WANG 2001 *Computational Mechanics*. Point interpolation method based on local residual formulation using radial basis functions (accepted).
20. M. J. D. POWELL 1992 in *Advances in Numerical Analysis* (F. W. Light, editors), 303–322. The theory of radial basis function approximation in 1990.
21. H. WENDLAND 1998 *Journal of Approximation Theory* **93**, 258–396. Error estimates for interpolation by compactly supported radial basis functions of minimal degree.
22. T. NAGASHIMA 1999 *International Journal for Numerical Methods in Engineering* **46**, 341–385. Node-by-node meshless approach and its application to structural analyses.
23. X. G. XU and G. R. LIU 1999 *Proceedings of APCOM'99 Fourth Asia-Pacific Conference on Computational Mechanics*, 1021–1026. A local-function approximation method for simulating two-dimensional incompressible flow.
24. C. A. BREBBIA, J. C. TELLES and L. C. WROBEL 1984 *Boundary Element Techniques*. Berlin: Springer Verlag.